Vol. 674: 73–88, 2021
https://doi.org/10.3354/meps13820

MARINE ECOLOGY PROGRESS SERIES
Mar Ecol Prog Ser

Published September 16

Lipid-related gene expression and sensitivity to starvation in *Calanus glacialis* in the eastern Bering Sea

Ann M. Tarrant[1,*], Lisa B. Eisner[2], David G. Kimmel[2]

[1]Woods Hole Oceanographic Institution, Woods Hole, MA 02543, USA
[2]NOAA Fisheries, Alaska Fisheries Science Center, Seattle, WA 98115, USA

ABSTRACT: In the eastern Bering Sea, lipid-rich copepods in the genus *Calanus* help to sustain productive fisheries and efficient energy flow through the ecosystem. In summer and autumn, *Calanus* populations consist primarily of stage C5 copepodites that are storing lipids and preparing for dormancy (diapause). We collected *Calanus* C5 copepodites from the eastern Bering Sea shelf in early autumn of 2015 and examined whether *Calanus* species composition, morphometric characteristics, and lipid-related gene expression varied along a north–south gradient. The sampled area exhibited marked differences in temperature, chl *a*, and *Calanus* abundance. However, the *Calanus* population was surprisingly homogeneous, composed almost entirely of *C. glacialis*, with no evidence for latitudinal trends in prosome size, oil sac fullness, or lipid-related gene expression. Rather than a latitudinal gradient, we found that *C. glacialis* from 1 southern station near the Pribilof Islands were larger and exhibited lower oil sac fullness and higher expression of lipid storage genes. Gene expression changes across stations were small relative to large shifts associated with shipboard feeding experiments. The similar characteristics of *C. glacialis* across stations imply that most of the C5 copepodites had experienced favorable growth conditions regardless of their latitudinal location. It remains unknown how environmental conditions affect *C. glacialis* physiology during other parts of their life cycle or how patterns vary among years. Continued studies of *C. glacialis* distribution, morphometrics, and gene expression could address these questions and serve as a harbinger for responses to future climatic changes.

KEY WORDS: Bering Sea · *Calanus* · Copepod · Lipid · Diapause · Genetics · Metabolism

1. INTRODUCTION

In temperate and polar marine ecosystems, large lipid-storing copepods in the genus *Calanus* are a key component of the mesozooplankton as well as important grazers of phytoplankton and microzooplankton. *Calanus* juveniles (copepodites) accumulate large lipid stores in an organ called the oil sac, which makes these copepods an energetically rich food source for fish, baleen whales, seabirds, and other predators (Lee et al. 2006, Falk-Petersen et al. 2009). The copepods use these lipids to survive periods of low food availability, sustain winter dormancy, and fuel adult reproduction (Hakanson 1984, Rey-Rassat et al. 2002, Lee et al. 2006, Saumweber & Durbin 2006, Halvorsen 2015). While *Calanus* species and populations vary in the extent to which sustained egg production is fueled by stored lipids versus concurrent spring feeding (Søreide et al. 2010, Daase et al. 2013), lipid accumulation by juveniles is critical to successful overwintering and overall food value to predators.

Calanus populations are a dynamic and important part of the food web along the broad (~500 km) and shallow (<200 m) shelf region in the eastern Bering Sea, where they help to support productive fisheries.

*Corresponding author: atarrant@whoi.edu

During the summer, *Calanus* can account for a majority of the diet of juvenile walleye pollock *Gadus chacogrammus* (Coyle et al. 2011, Strasburger et al. 2014, Duffy-Anderson et al. 2017, Andrews et al. 2019). The walleye pollock fishery in the eastern Bering Sea is the largest commercial fishery by mass in the USA (Fissel et al. 2017, National Marine Fisheries Service 2020). *Calanus* abundance also varies spatially, both along and across the shelf, with *Calanus* found primarily on the middle and outer shelves (50–200 m bathymetry) in late summer (Eisner et al. 2018). Spatial patterns in *Calanus* abundance and overall zooplankton community composition correspond to differences in seasonal ice cover as well as bottom water temperature and salinity (Eisner et al. 2014, 2018). *Calanus* undergoes diel vertical migration within the Bering Sea (Schabetsberger et al. 2000, Miksis-Olds et al. 2013). At a station near the Pribilof Islands sampled in September 1996, the *Calanus* population was broadly distributed throughout the water column at night and concentrated at around 30 to 40 m during the day (Schabetsberger et al. 2000). By late summer and early autumn, *Calanus* populations in the eastern Bering Sea are composed mainly of late-stage juveniles (fifth copepodite, C5 stage, the last juvenile stage), particularly in cold years (Eisner et al. 2018, Kimmel et al. 2018). In the typical view, these juveniles descend close to the seafloor during late autumn and overwinter in a dormant state called diapause (e.g. Baier & Napp 2003, Coyle & Gibson 2017). Alternatively, recent studies conducted in Arctic fjords indicate that *Calanus glacialis* may continue to feed on microzooplankton and other prey throughout the winter (Cleary et al. 2017, Hobbs et al. 2020). In either case, Bering Sea populations of *Calanus* mature to adults prior to the spring bloom. In the eastern Bering Sea, *Calanus* is thought to produce 1 generation per year (Baier & Napp 2003, Banas et al. 2016).

Interannual variation in the abundance of large copepods in the eastern Bering Sea has been attributed to differences in the extent of winter ice cover and the timing of ice retreat as well as the effects of these phenomena on temperature, stratification, nutrient availability, and primary production (Coyle & Gibson 2017, Eisner et al. 2018, Kimmel et al. 2018, Hunt et al. 2020, Lomas et al. 2020). In cold, high ice years, there is typically an earlier spring bloom associated with the sea ice, whereas low ice years are characterized by later open-water spring blooms (Sigler et al. 2014). High ice years are also associated with a more extensive cold pool (<2°C) of bottom water that persists through the summer (Grebmeier et al. 2006, Stabeno et al. 2012, Duffy-Anderson et al. 2017). The timing and extent of sea ice coverage are key predictors of *Calanus* abundance, presumably due to effects of ice cover on the availability of ice algae and microzooplankton to support spring reproduction following diapause emergence (Hunt et al. 2020). In this region, it is less clear to what extent conditions later in the year affect *Calanus* physiology, entry into diapause, and overwintering success.

The 2 primary *Calanus* species in the Bering Sea ecosystem are *C. marshallae*, endemic to the subarctic Pacific, and *C. glacialis*, an arctic specialist particularly adapted to shelf environments (Frost 1974). Because these species are difficult to distinguish morphologically, ecological studies often treat *C. marshallae* and *C. glacialis* as a functional taxonomic unit (e.g. Plourde et al. 2005, Eisner et al. 2014). However, genetic markers can distinguish these species (Bucklin et al. 1995, Smolina et al. 2014) and have the potential to provide valuable insight into the ecological dynamics of each, such as distributional shifts that are anticipated to result from climate change (Coyle et al. 2011, Eisner et al. 2014, Hunt et al. 2020). A similar approach has been used to discriminate genetic lineages within *C. glacialis* (Nelson et al. 2009). In contrast to these phylogenetic approaches, application of molecular methods to physiological studies of *Calanus* has been limited. For *C. glacialis,* measurements of gene expression have been used in the context of controlled experiments to examine responses to acidification (Bailey et al. 2017), thermal stress (Smolina et al. 2015), and petroleum-based pollutants (Hansen et al. 2013).

Beyond characterizing physiological responses in controlled lab experiments, gene expression measurements can be used to investigate the physiological condition of natural copepod populations. Most notably, a study of *Neocalanus flemingeri* within the Gulf of Alaska revealed geographic variation in expression of metabolic genes that was associated with environmental gradients in food availability (Roncalli et al. 2019). In addition, a few studies have identified genes that might be developed into markers of lipid metabolism in the North Atlantic copepod *C. finmarchicus* (Tarrant et al. 2008, 2014, Lenz et al. 2014). Among these, a fatty acid elongase (ELOV) and a fatty acid binding protein (FABP) have been proposed as markers of lipid accumulation within the C5 stage. Another potential target for biomarker development is the glycerol-3-phosphate acyltransferase (GPAT) family, which includes both mitochondrial and microsomal enzymes. GPAT activity is the rate-limiting step in triacylglycerol synthesis in mammals (Wendel et al. 2009). Additional genes could serve as

catabolic markers, reflecting both digestive processes and the utilization of energetic stores; these include lipases, phosphoenolpyruvate carboxykinase (PEPCK), and pyruvate dehydrogenase kinase (PDK). Lipases are enzymes that cleave the ester bonds found in neutral lipids, an essential step in metabolizing lipids either in food particles within the digestive tract or stored within cells (Rivera-Pérez 2015). While intracellular lipases can have broad substrate affinity, they are primarily associated with triacylglycerol metabolism, and an intracellular lipase isolated from shrimp has been shown to metabolize triacylglycerol substrates (Rivera-Pérez et al. 2011). In *C. glacialis,* wax ester is the primary lipid form in the oil sac, but smaller amounts of triacylglycerol occur throughout the body and represent a short-term labile energy source (Lee et al. 2006, Mayzaud et al. 2016). Thus, intracellular lipase expression may be sensitive to short-term changes in energetic condition. PEPCK is the rate-limiting enzyme in gluconeogenesis, the pathway that produces glucose from lipids, and PDK helps to regulate the relative rates of glucose and fatty acid oxidation. Both PEPCK and PDK can be induced by starvation in the fruit fly *Drosophila melanogaster* (Palanker et al. 2009). PEPCK is upregulated during diapause in many insect species (Poelchau et al. 2013, Spacht et al. 2018) and during early stages of diapause in *C. finmarchicus* (Häfker et al. 2018a,b).

For this study of the *Calanus* population on the eastern Bering Sea shelf, we took advantage of a multidisciplinary oceanographic cruise that sampled zooplankton along the 70 m isobath north–south transect in late summer and early autumn of 2015. We had several objectives, the first of which was to determine the species composition of the *Calanus* population within this region. We hypothesized that a mix of *C. marshallae* and *C. glacialis* would be found, with an increasing proportion of *C. glacialis* present in the northern portion of the transect; we tested this hypothesis using genetic methods. Next, we wanted to compare the relationship between oil sac volume and prosome length as an indication of relative lipid accumulation or fullness (Miller et al. 2000). We predicted that a gradient in size would exist, where smaller individuals would be present in the south and larger individuals in the north. We further predicted that though the oil sac volume would be smaller in the south, the oil sac volume and prosome length would be proportional along the transect. These hypotheses are based on lower temperatures being associated with slower developmental rates and larger body size (Kiørboe & Hirst 2008, Evans et al. 2020). Alternatively, we considered it possible that patchiness in food availability would result in spatial variability in oil sac fullness. Finally, we wanted to determine if a suite of lipid metabolic markers showed differential expression within a *Calanus* species along the gradient. We hypothesized that lipid-related gene expression would correlate with oil sac fullness. To further examine the expression of these lipid metabolic genes, we conducted feeding experiments with wild-caught *C. glacialis* to determine how their expression changed over time for fed and starved individuals.

2. MATERIALS AND METHODS

2.1. Hydrographic and zooplankton sampling

Shipboard sampling was conducted as part of a multi-disciplinary survey over the eastern Bering Sea shelf in late summer and early fall of 2015. Measurements of hydrographic properties and chl *a* concentration are described and reported by Duffy-Anderson et al. (2017). Briefly, the region was characterized by warm water in the south and a substantial subsurface cold pool in the north (see also Figs. 1 & 3). Along the 70 m isobath, integrated chl *a* was patchy with generally higher values in the south, and stations with higher integrated chl *a* also had a greater proportion of large (>10 µm) phytoplankton (Duffy-Anderson et al. 2017).

For this study, *Calanus* C5 copepodites were sampled from 92 stations along the 70 m isobath from 55.0° to 62.4° N in the eastern Bering Sea from 6 September to 4 October 2015 (Fig. 1). At each station, zooplankton were collected through oblique tows from near the surface to within 5 to 10 m of the bottom using paired bongo nets (Kimmel et al. 2018). These tows were retrieved during daytime between 08:45 and 16:07 h (UTC−11, corresponding to the astronomical correction at 165° W). For reference, on 27 September 2015 at 59° N, 169° W, sunrise was at 06:12 h and sunset at 18:01 h UTC−11. A portion of each tow was preserved in 5% buffered formalin in seawater. Copepods were identified to the lowest taxonomic level and stage possible at the Plankton Sorting and Identification Center (Szczecin, Poland) and verified at the NOAA Alaska Fisheries Science Center (Seattle, Washington, USA). *Calanus marshallae* and *C. glacialis* were reported as a single taxonomic unit.

From 5 focal stations (Table 1), *Calanus* individuals were picked from the larger 60 cm, 505 µm mesh net and photographed at 50× magnification using a Canon EOS-20D camera attached to a Zeiss Stemi 2000C

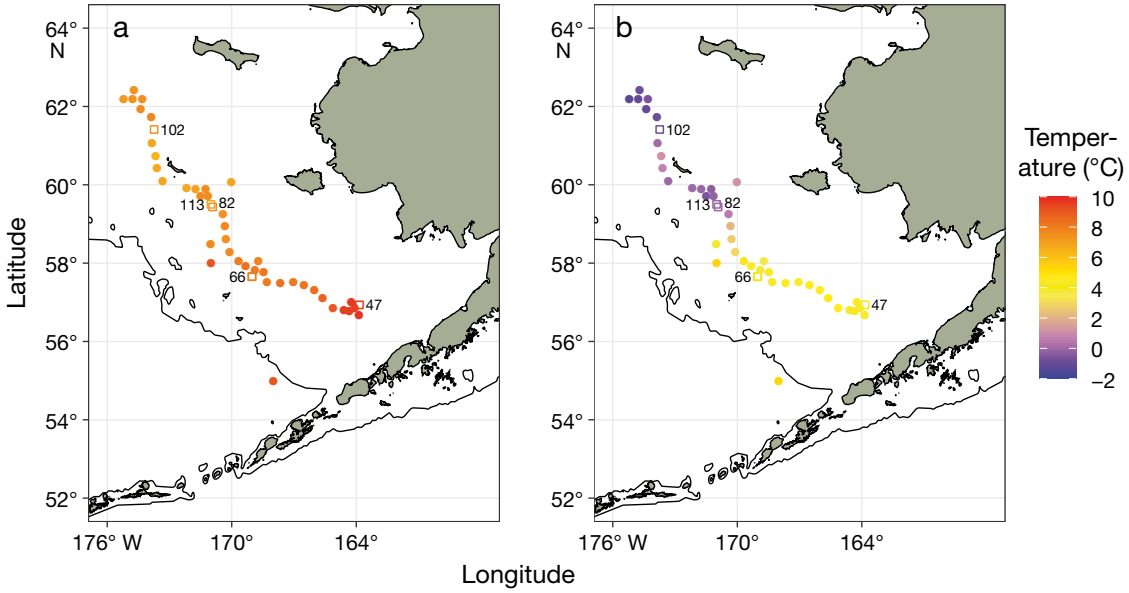

Fig. 1. (a) Surface (0–5 m) and (b) bottom (5 m above bottom) water temperature for each station in September to October 2015. The cruise track follows the 70 m isobath of the eastern Bering Sea shelf, west of the Alaskan mainland. The solid black line is the 200 m isobath, indicating the shelf edge. Numbers and open squares indicate focal stations for molecular studies of *Calanus glacialis*

Table 1. Focal stations sampled for molecular studies of *Calanus* C5 copepodites in 2015. The official time zone for Alaska and the US Bering Sea is UTC-9; however, the time zone designation is irregularly shaped. UTC-11 corresponds to the astronomical correction at 165° W. Stn 113 was used for genetic species ID only; no gene expression measurements were made.

Stn	Local date	UTC	UTC-11	Depth (m)	Location
47	24 Sep	17:45	08:45	69	56° 56.07′ N, 163° 50.71′ W
66	25 Sep	21:52	12:52	69	57° 39.31′ N, 169° 1.78′ W
82	26 Sep	21:02	12:02	73	59° 26.10′ N, 170° 54.57′ W
102	28 Sep	19:46	10:46	76	61° 24.63′ N, 173° 44.17′ W
113	29 Sep	7:07	16:07	74	59° 30.09′ N, 170° 59.93′ W

stereomicroscope. To calibrate measurements, photographs were taken of a stage micrometer at the start of each sampling session. Copepods were then either preserved for molecular analysis (RNAlater) or frozen for lipid measurements. The data from the lipid analysis were deemed unreliable due to losses during sample concentration and anomalously high proportions of polar lipids. The lipid results are not discussed further; however, photographs of these copepods were included in the morphometric analyses (described in Section 2.3).

2.2. Shipboard feeding experiments

Additional C5 copepods from Stns 66 and 82 were used in shipboard feeding experiments. The copepods were incubated in 1 l wide-mouth polypropylene bottles filled with 0.22 µm filtered seawater at a density of 15 to 20 copepods l^{-1}; similar densities have been used in several previous physiological studies of *C. glacialis* and *C. finmarchicus* (Stevens et al. 2004, Tarrant et al. 2014, Thor et al. 2016). The bottles were randomly divided between fed and starved treatments that were sampled after 3 or 7–9 d (short and long incubations, respectively). For fed treatments, a mixed assemblage of microplankton was obtained by passing a gentle stream of surface seawater over a partially submerged 20 µm sieve. The filtrate from 20 l of seawater was resuspended in 0.5 l of filtered seawater (concentrated 40-fold). Every 1 to 2 d, 100 ml of water was removed from each experimental bottle using a 50 ml wide-bore pipette. Bottles in the fed treatments were given 100 ml of freshly collected microplankton solution, nominally resulting in a 4-fold enrichment relative to surface seawater. Bottles in the starved treatments were given an equivalent volume of filtered seawater. Copepods in the long incubations were gently transferred into fresh bottles using a ladle midway through the experiment. Bottles were covered with black plastic sheeting and incubated in an outdoor tank with flowing surface seawater. Based on modeled copepod oxygen con-

sumption rates (Ikeda et al. 2001), oxygen saturation state was predicted to remain above 90% during all incubations. As copepods were sampled from the experiments, they were photographed and preserved (as described in Section 2.1).

2.3. Morphometric analysis

The prosome length, prosome width, and oil sac area were estimated from digital photographs as described previously (Tarrant et al. 2008). Oil sac volume was estimated from area by assuming the oil sac to be a cylinder of varying thickness, summing unit cylindrical cross sections across its length, and using an empirically derived polynomial to adjust estimates for asymmetry (Miller et al. 2000, Tarrant et al. 2008). Oil sac volume was also estimated using a more recently developed exponential function (Vogedes et al. 2010). The size-dependent apparent maximum oil storage capacity was determined empirically from all available photographs (n = 378; Table S1 in Supplement 1 at www.int-res.com/articles/suppl/m674p073_supp1.xlsx [for Tables S1, S2 & S4], Fig. S1 in Supplement 2 at www.int-res.com/articles/suppl/m674p073_supp2.pdf [for Tables S3, S5 & S6, Figs. S1–S4]) using the curve-fitting approach described by Miller et al. (2000), giving the equation:

$$\text{Max volume } (\text{mm}^3) = [\text{Prosome length (mm)} \times 0.588] - 1.255$$

The presence or absence of food within the gut was determined visually from the photographs.

2.4. Candidate genes

Candidate genes associated with lipid storage (FABP, ELOV, GPATa, and GPATb) were selected based on their known roles in other organisms and/or expression patterns in *C. finmarchicus* (Tarrant et al. 2008, 2014, Lenz et al. 2014). Three additional genes, PEPCK, PDKa, and a lipase (hereafter 'Lipase'), were chosen to indicate gluconeogenesis and lipid catabolism. Candidate reference genes for normalization of quantitative PCR (qPCR) measurements were selected based on their stability in previous studies with *C. finmarchicus* (UBX, TSG, EF1a; Tarrant et al. 2014). *C. finmarchicus* sequences were identified from previous studies (as above) and through blastx searches of a *C. finmarchicus* transcriptome (GBFB00000000.1) with reference sequences from human, mouse, *Drosophila melanogaster*, or other taxa (Table S2). *C. glacialis* sequences were then identified by using *C. finmarchicus* sequences to query *C. glacialis* transcriptomic databases (Ramos et al. 2015, Smolina et al. 2015), and homology was inferred on the basis of reciprocal tblastn searches. In some cases, mammalian sequences were used to directly query the *C. glacialis* databases. To verify the transcript predictions, portions of each gene, including the amplicon used in subsequent assays, were amplified, cloned, and sequenced.

2.5. Nucleic acid extraction, 16S, and qPCR

Total RNA was extracted from individually preserved C5 copepodites using the Aurum Fatty and Fibrous Tissue Kit (Bio-Rad) with on-column DNAse treatment, as we have done previously (Tarrant et al. 2008). RNA yield and purity were assessed using a Nanodrop spectrophotometer. Complementary DNA (cDNA) was synthesized from 210 or 300 ng total RNA (depending on yield) in 20 µl reactions using the iScript cDNA Synthesis Kit (Bio-Rad). Water was subsequently added to the cDNA to create a concentration equivalent to 9 ng RNA template per µl.

To distinguish between *Calanus* species, a portion of the 16S rRNA gene was amplified using primers 16SAR (Palumbi & Benzie 1991) and 16SB2R (Lindeque et al. 2006). For 16S amplification, 1.5 µl of cDNA template was added to a cocktail containing 0.2 mM dNTPs, 10 µM primers, and 1 U HotMaster *Taq* DNA polymerase (Quanta Bio) in a 20 µl reaction with the provided buffer. Cycling conditions were 94°C for 1 min, 35 cycles (of 94°C for 5 s, 45°C for 30 s, 72°C for 1 min), and 72°C for 5 min. PCR products were visualized on agarose gels, purified using the MinElute Gel Extraction Kit (Qiagen), and directly sequenced. *C. glacialis* were distinguished from *C. marshallae* on the basis of a diagnostic single nucleotide polymorphism within the amplicon. Only genetically confirmed *C. glacialis* samples were used in gene expression analysis.

For qPCR reactions, all primer sequences are given in Table 2. The 20 µl reaction mix consisted of 10 µl i*Taq* Universal SYBR Green Supermix (Bio-Rad), 0.5 µM primers, and 1 µl cDNA. Samples were analyzed in single wells of a 96-well plate on an iCycler iQ Real-Time PCR Detection System (Bio-Rad). Cycling conditions were 95°C for 1 min followed by 40 cycles (of 95°C for 15 s and 60°C for 25 s). Melt curve analysis was conducted to ensure that only a single specific product was amplified. Amplification efficiency was initially tested for each primer set using a serially diluted cDNA sample. Gene expres-

Table 2. Genes measured in quantitative PCR assays and associated primer sequences. Sequences beginning with HACJ from Ramos et al. (2015); those beginning with GBXT from NCBI BioProject PRJNA237014. F: forward; R: reverse

Gene and Accession no.	Primer sequence
ELOV	F: 5′-CGT GCA CGT GGT CAT GTA TTT C-3′
HACJ01034268	R: 5′-AGC TGC ATG CTG GTG ATG TAC C-3′
FABP	F: 5′-TGC AAA TGG CAG GAA GCT ACA C-3′
HACJ01042517	R: 5′-CCT TCC TCA GGA TGA ACC CAA C-3′
GPATa	F: 5′-CCC AAG GGT GGT ATC TGT GTG-3′
GBXT01013094	R: 5′-CCT CCA TGT TTC TGC CCA GTC-3′
GPATb	F: 5′-GGA GAA GGT GAG AAT GCG ATT G-3′
HACJ01012519	R: 5′-TTC CGT CCC ACA GAA GAT CAA C-3′
Lipase	F: 5′-CAA TGG TTG GTC ACA AGT GC-3′
HACJ01015115	R: 5′-ACA ATC CTC TCC CTC GAA GC-3′
PEPCK	F: 5′-AAC CTG GCA ATG ATG AGT CC-3′
HACJ01003961	R: 5′-GCC CTC AGT TGT CCA TTA GC-3′
PDKa	F: 5′-ATG CTC ATC CAT CAG CAC AC-3′
GBXT01017260	R: 5′-TGA TGA CGG ACT TGA CCT TG-3′
EF1a	F: 5′-GAT GCA CCA CGA GTC TCT CC-3′
GBTX01021598	R: 5′-GGC TTG TTC TTG GAG TCG GA-3′
TSG	F: 5′-AGC CTC CAG TAT CGG TTC AG-3′
GBXT01002122	R: 5′-TGG TTC TGG CTG AAG TCC TC-3′
UBX	F: 5′-TGA GGG TCT CCA CAC ACA AC-3′
GBXT01019969	R: 5′-ACA GCT GGA AGG AGA GCA AG-3′

sion (threshold amplification cycle reported in relative fluorescence units) was calculated in samples using LinRegPCR v2016.1, which directly estimates amplification efficiency within each sample (Ramakers et al. 2003).

2.6. Statistical design and analysis

Gene expression values were $\log_2$ transformed and normalized by EF1a, which did not vary by station or experimental treatment. Expression of FABP, ELOV, GPATa, and GPATb was measured in all copepod samples, and expression of PEPCK, PDKa, and Lipase was measured in a subset of samples. From each of 4 stations, expression was measured in 6 to 10 freshly collected copepods, depending on the gene (n = 10: FABP, ELOV, GPATa, GPATb, EF1a; n = 6–7: PEPCK, PDKa, Lipase), i.e. expression of either 5 genes or all 8 genes was measured for each copepod individual. Within the experiment, expression was measured in 8 to 11 (FABP, ELOV, GPATa, GPATb, EF1a) or 4 to 9 (PEPCK, PDKa, Lipase) copepods per treatment; as with the field-collected animals, expression of either 5 or 8 genes was measured for each individual. Gene expression in the experimental animals was compared with expression in the field-collected animals from the same sites (field group, n = 20: FABP, ELOV, GPATa, GPATb, EF1a; n = 12: PEPCK, PDKa, Lipase).

Even after transformation, gene expression data exhibited heteroscedasticity. Morphometric measurements and gene expression were compared among stations (field samples) or treatments (experiment) using 1-way Welch's ANOVA, as implemented in R v4.0.2 (R Core Team 2020). For measurements with significant differences ($p < 0.05$), post hoc comparisons were made using the Games-Howell test, within the userfriendlyscience R package (Peters 2018). In field samples, relationships among genes were examined using Spearman's rank-based correlations and visualized using the rcorr() function in the Hmisc R package (Harrell & Dupont 2006). For field samples, gene expression patterns of ELOV, FABP, GPATa, and GPATb were visualized using non-metric multidimensional scaling (nMDS) using the metaMDS function within the vegan package (Oksanen et al. 2019). For nMDS analysis, $\log_2$-transformed, normalized gene expression was multiplied by −1; analysis was then conducted based on Euclidean distances in 2 dimensions with 20 random restarts.

3. RESULTS

3.1. Station comparison and species determination

Surface temperature, bottom temperature, and integrated chl *a* all increased from north to south (Figs. 1 & 2; depth-specific chl *a* shown in Fig. S2). Within the upper mixed layer, the southernmost focal station (Stn 47) was much warmer than the other focal stations (9.6°C vs. 6.7–8.0°C). Below the thermocline, temperatures were sharply distinguished between the 2 southern (Stns 47 and 66) and 3 northern (Stns 82, 102, and 113) focal stations (4.0–5.0°C south vs. −0.7 to 0.1°C north; Fig. 3). The cold bottom water in the northern stations is characteristic of the cold pool associated with sea ice presence during the prior winter. Integrated chl *a* was much higher in the southernmost focal station (>6 vs. <2 µg l^{-1}; Fig. 3), which is consistent with the previously reported trend of higher chl *a* in the south during this survey.

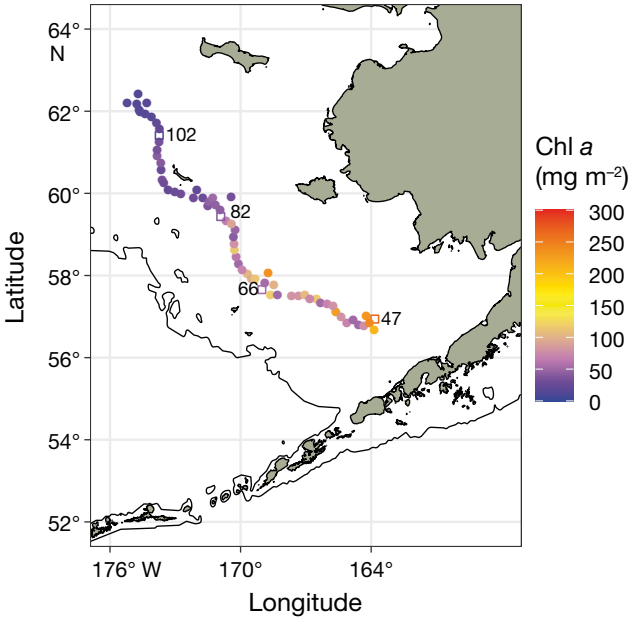

Fig. 2. Integrated chl *a* for each station in September to October 2015. The cruise track follows the 70 m isobath of the eastern Bering Sea shelf, west of the Alaskan mainland. The solid black line is the 200 m isobath, indicating the shelf edge. Numbers and open squares indicate focal stations for molecular studies of *Calanus glacialis*. Integrated chl *a* measurements were not made at Stn 113

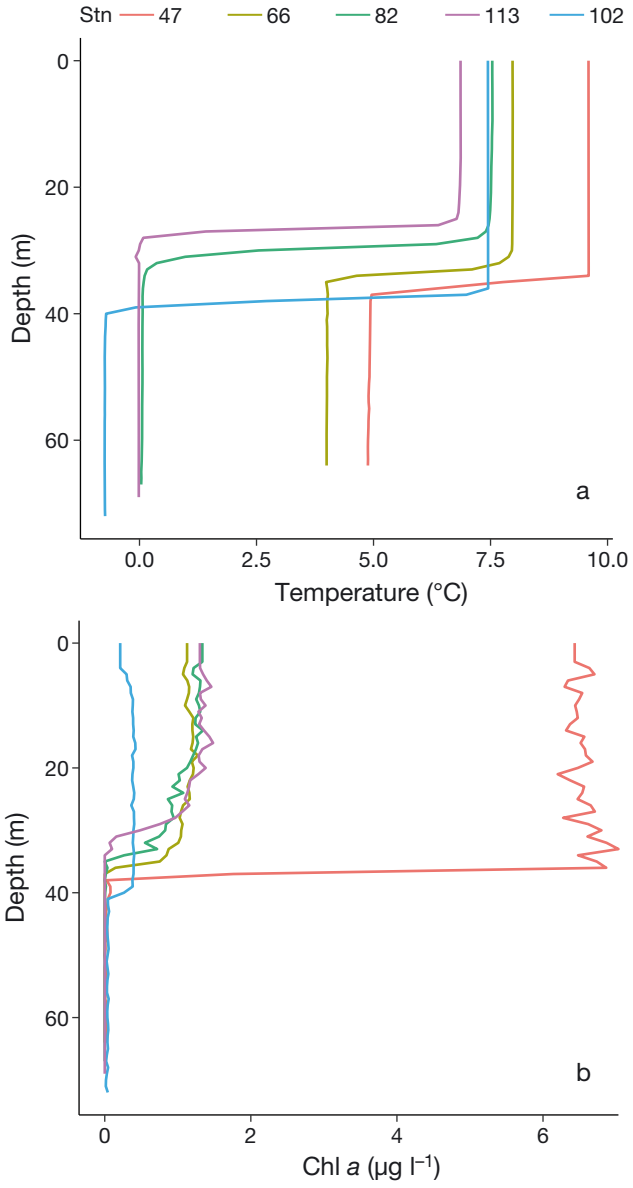

Fig. 3. Profiles of (a) temperature and (b) chl *a* in September 2015 at focal stations for molecular studies of *Calanus glacialis*. Stations are listed from south (47, left) to north (102, right); see also Fig. 1 for locations

At most stations, including all 5 focal stations, *Calanus* were overwhelmingly in the C5 stage (>95%, data not shown). Along the 70 m isobath, 2 peaks of abundance occurred within the central portion and northern end of the track (Fig. 4). The temperature and salinity characteristics (water column means) along the isobath formed 2 distinct clusters, with high copepod abundance associated with colder and fresher water (Fig. 5). Consistent with this, abundance was much higher in the northern focal stations, with a >10-fold difference between Stn 82 and the 2 southern focal stations (Stns 47 and 66) (Table 3). Copepods from all focal stations were actively swimming, and food visible in the guts of some specimens indicated recent feeding. Low chl *a* throughout the water column at 1 northern station (Stn 102) was matched by a small proportion of copepods with food visible in their guts.

A total of 106 *Calanus* individuals, including all those that were used for gene expression analysis, were classified to species through sequencing of the 16S genetic marker, which indicated that 104 of 106 individuals were *Calanus glacialis* (Table 3). Two individuals, both collected from 1 northern station (Stn 113), were identified as *C. marshallae*; no gene expression analysis was conducted on animals from this station. Morphometric measurements were derived from images of confirmed *C. glacialis* as well as images without genetic confirmation.

3.2. Morphometrics

Measurements of all field-collected copepods are contained in Table S1 with means by stations displayed as boxplots in Fig. 6. Estimates of oil sac volume produced by 2 methods were highly correlated (r = 0.993) and did not differ among stations in either

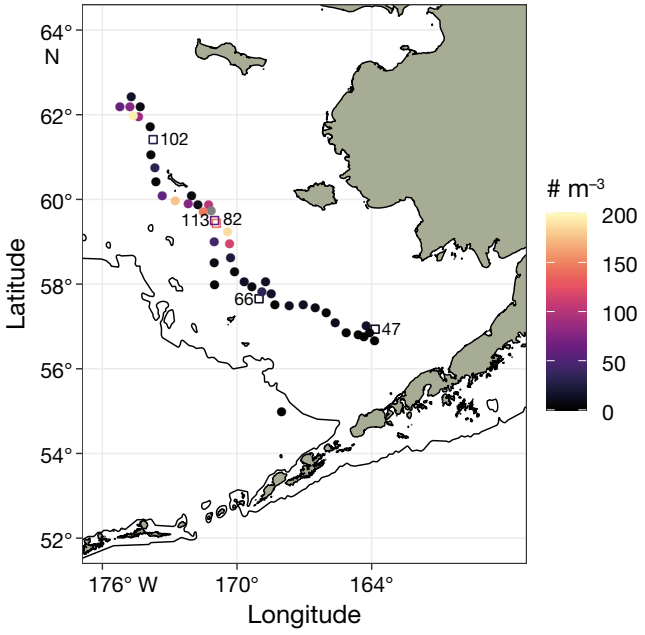

Fig. 4. *Calanus* C5 mean water column abundance in September to October 2015. The cruise track follows the 70 m isobath of the eastern Bering Sea shelf, west of the Alaskan mainland. The solid black line is the 200 m isobath, indicating the shelf edge. Numbers and open squares indicate focal stations for molecular studies of *Calanus glacialis*

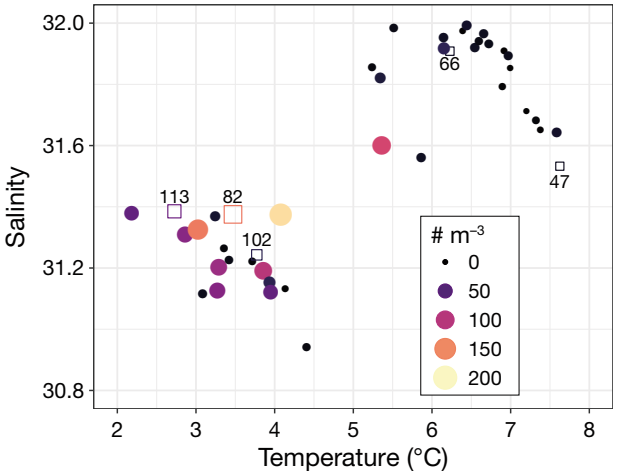

Fig. 5. Temperature salinity plot showing waters where *Calanus* C5 had the highest mean water column abundance along the 70 m isobath of the eastern Bering Sea in September to October 2015. Salinity and temperatures are water column means. Numbers and open squares indicate focal stations for molecular studies of *Calanus glacialis*; Stns 47 and 66 were the southernmost of these

case (cross-sectional area method: $p = 0.54$, Fig. 6b; exponential method: $p = 0.44$, not shown).

Calanus from southern Stn 66 had longer prosomes than those from southern Stn 47 as well as northern Stn 102 ($p < 0.001$ in both cases, Games-Howell test, Table S3, Fig. 6a). While *Calanus* from Stn 47 were relatively small, the volume of the oil sac was not significantly different from other focal stations; therefore, their fractional fullness at Stn 47 was significantly higher than that at Stns 66 and 82 (Stn 47 vs. 66 $p < 0.01$, Stn 47 vs. 82 $p = 0.009$, Games-Howell test; Table S3, Fig. 6c). The same trends were apparent when the data set was restricted to genetically confirmed *C. glacialis* specimens (i.e. the subset of genetically confirmed animals that were sampled directly from the field and not used in experiments), but the sample size was smaller (n = 9–10), and the differences were not statistically significant (data not shown).

3.3. Identification of *Calanus glacialis* transcripts

Accession numbers for measured transcripts are given in Table 2 and for all identified homologs in Table S4. Among the genes related to lipid storage, homologs of 1 *C. finmarchicus* FABP transcript and each of 4 ELOV transcripts were identified in *C. glacialis*. One putative mitochondrial GPAT and 4 microsomal GPATs were identified in *C. finmarchicus*, and

Table 3. *Calanus* C5 copepodite mean water column abundance, genetic species confirmation, and numbers with visible food or no food in their guts. *Calanus glacialis* ID includes some animals that were used in experiments and thus not photographed upon collection. Total field photographs include animals used in molecular studies and for other purposes. Percentage of animals with visible food is based relative to the total number of field photographs. Inability to determine food was because either the focus on the gut was poor or dark patches were observed that might or might not have been food

Stn	Abundance (C5 m^{-3})	Genetic ID as *C. glacialis*	Total no. of field photographs	Food visible	No food	Unable to determine
47	12.48	10/10 (100%)	36	23 (64%)	2	11
66	14.01	29/29 (100%)	43	21 (49%)	14	8
82	142.76	26/26 (100%)	10	4 (40%)	5	1
102	30.60	20/20 (100%)	40	5 (13%)	23	12
113	64.05	19/21 (90%)	11	9 (90%)	1	1

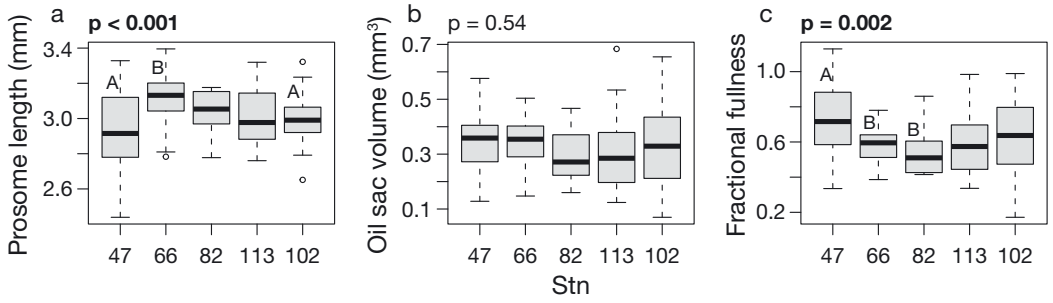

Fig. 6. Morphometric analysis — (a) prosome length, (b) oil sac volume, (c) fractional fullness — of *Calanus* C5 copepodites freshly sampled from the field, including animals used for both gene expression and lipid measurements (n = 10–40 per station; 140 total animals). Stations are listed from south (47, left) to north (102, right); see also Fig. 1. Boxplots show the first and third quartiles, with a line showing the median, and open circles represent outliers. Measurements were compared across stations with 1-way Welch ANOVA, and p-values are shown at the top of each plot with significant results ($p < 0.05$ shown in bold). Stations exhibiting significant differences in post-hoc comparisons (Games-Howell test $p < 0.05$) are indicated by different uppercase letters. Fractional fullness (c) was calculated by manually fitting a line to the maximum observed size-dependent oil storage capacity (Fig. S1, see Section 2.3 for further details)

homologs of two of the microsomal forms were detected in *C. glacialis* (arbitrarily designated GPATa and GPATb).

Identification of catabolic genes focused on intracellular lipases, PEPCK, and PDK. Two putative intracellular lipases were identified in *C. finmarchicus*, and a homolog for one of these was identified in *C. glacialis*. Two PEPCK transcripts were identified in *C. finmarchicus*, but these differed mainly in length and had nearly identical sequences. The longer sequence retrieved several highly similar *C. glacialis* sequences. Multiple PDK transcripts were identified in both *C. finmarchicus* and *C. glacialis*. Several of the *C. glacialis* sequences were highly similar, with long stretches of identical predicted amino acid sequences. Primers were developed for 3 transcripts with different predicted amino acid sequences and tested in a small number of samples (not shown). The primer set used in subsequent analyses (targeting PDKa) was chosen based on assay quality parameters (melt curve analysis, amplification efficiency) and high apparent expression (low threshold cycle).

Three genes (ELOV, FABP, and GPATb, Fig. 7a,b,d, respectively, Table S5) exhibited significant differences in expression among focal stations, and all 3 showed a trend for higher expression at Stn 66 relative to Stns 47 and 102. For both ELOV and FABP, expression was significantly higher at Stn 66 than at Stns 47 and 102. FABP expression was also significantly higher at Stn 82 than at Stn 102. GPATb expression was significantly higher at Stn 66 than at Stn 102. The other genes did not show any significant differences, although PEPCK was variable with some particularly high values at Stn 102. Overall, several genes showed correlated expression patterns within the field samples (Fig. 8). The strongest relationships were positive correlations of FABP with ELOV and GPATb, a positive correlation of PEPCK with Lipase, and negative correlations of PEPCK with FABP, ELOV, and GPATb. To visualize overall patterns in gene expression, nMDS was conducted using the expression of the 4 genes (ELOV, FABP, GPATa, GPATb) that were measured in the full set of 40 field-collected copepods (Fig. 9). This analysis discriminated Stn 66 from Stns 47 and 102. ELOV was negatively correlated with oil sac volume and fractional fullness, with a pattern of low ELOV in the most lipid-rich copepods from Stns 47 and 102 (Fig. S3). No other relationships between morphological and molecular measurements were statistically significant.

3.4. Feeding experiments

Short (3 d) and long (7–9 d) feeding experiments were conducted with copepods from Stns 66 and 82. Samples from the 2 sites were pooled because field-collected animals exhibited no differences in gene expression or morphology (Figs. 6 & 7). GPATa, PDKa, and Lipase exhibited no significant differences in expression (Table S6, Fig. S4). Among the other genes, the largest differences were associated with time in captivity rather than the feeding treatments (Fig. 10), which implies that the feeding conditions were suboptimal. As in the field study (Fig. 7), expression patterns of ELOV, FABP, and GPATb were broadly similar to one another and opposite of the PEPCK pattern. FABP expression rapidly declined in all of the experimental treatments, which may indicate that this gene is the most sensitive to changes in feeding activity. ELOV and GPATb expression declined more slowly. After 3 d, ELOV and GPATb ex-

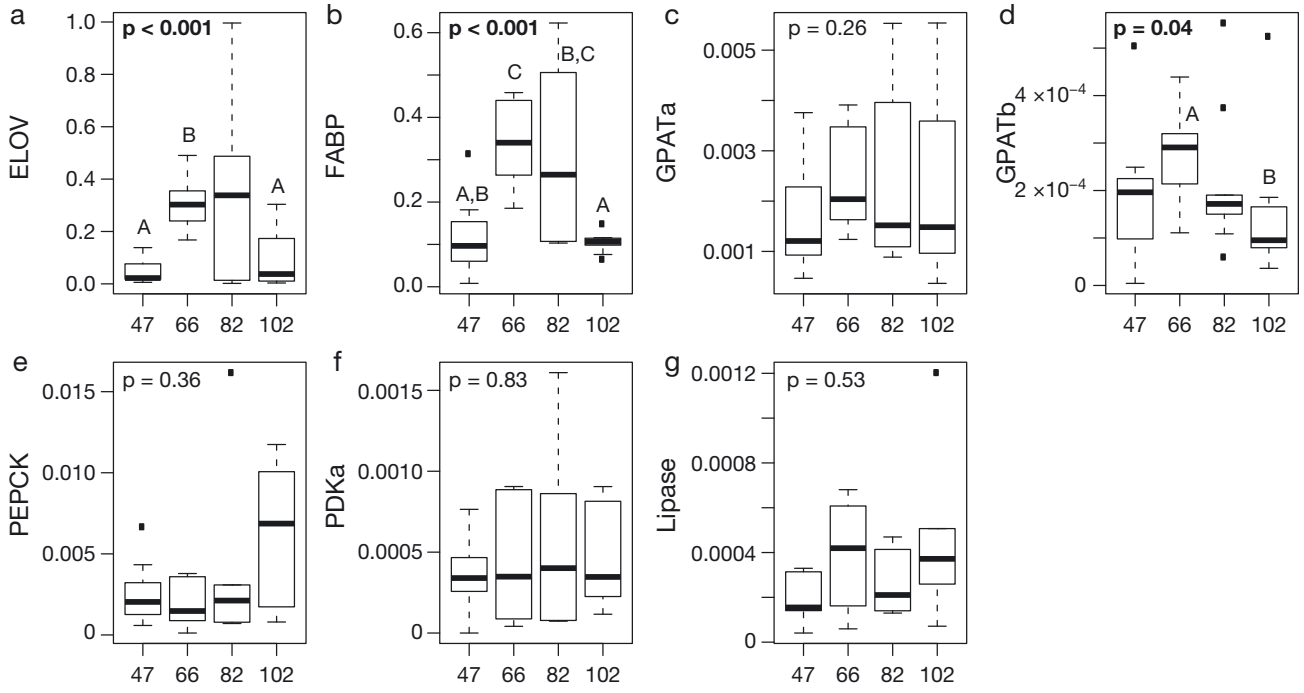

Fig. 7. Relative gene expression (log_2-transformed, normalized relative fluorescence units) by station in field-collected *Calanus glacialis* C5 copepodites (n = 6–10 per station, gene expression was not measured at Stn 113). Genes analyzed are (a) ELOV, (b) FABP, (c) GPATa, (d) GPATb, (e) PEPCK, (f) PDKa, and (g) Lipase. Stations are organized from south (47, left) to north (102, right). Boxplots show the first and third quartiles, with a line showing the median, and solid squares represent outliers. Expression was compared among stations using 1-way Welch ANOVA, and p-values are shown within the plot area (significant values, $p < 0.05$, indicated in bold). Significantly different pairs of stations ($p < 0.05$), as identified through Games-Howell post hoc comparisons, are indicated with different uppercase letters

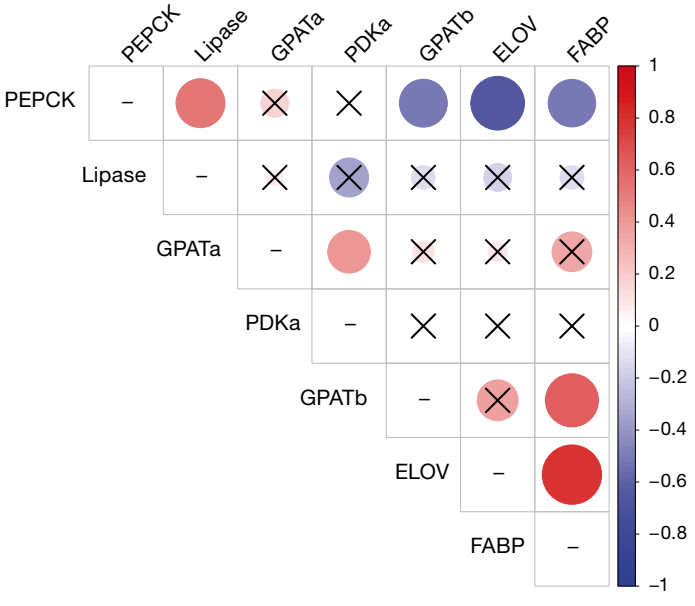

Fig. 8. Matrix indicating correlations (Spearman ranks) among pairs of genes in field-collected *Calanus glacialis* C5 copepodites (n = 40 per gene). The strength of the correlation is indicated by both size and color. ×: comparisons with non-significant comparisons ($p > 0.05$)

pression in fed animals was not significantly different from the field. Expression of these 2 genes showed a decreasing trend in starved animals, with a significant difference between the 3 d starved and field-collected animals for GPATb. With a smaller sample size, PEPCK did not show any significant differences after 3 d, but the trend was toward increased expression in starved animals. After 7 to 9 d, there were no significant differences between the fed and starved animals for any of the measured genes. Expression of FABP remained low, ELOV and GPATb dropped relative to the field and 3 d samples, and PEPCK rose relative to these groups.

4. DISCUSSION

The overall goal of this study was to determine if *Calanus* species composition, morphometric characteristics, and lipid metabolic markers varied along a north–south gradient in the eastern Bering Sea. Given the recent lack of ice in the Bering Sea (Stabeno & Bell 2019) and projected future warming (Hermann et al. 2019), knowledge of potentially differing

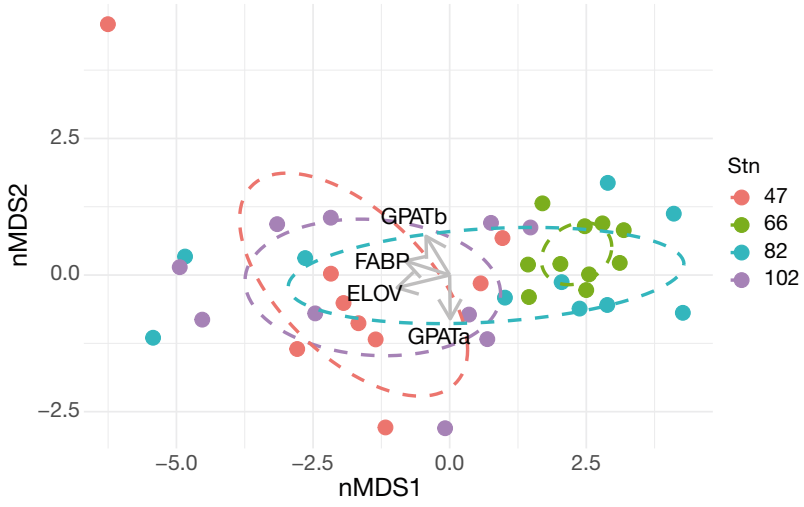

Fig. 9. Non-metric multidimensional scaling (nMDS) plot based on Euclidean distances among *Calanus glacialis* C5 copepodite samples for expression of lipid synthesis genes (FABP, ELOV, GPATa, and GPATb). Analysis parameters: 2 dimensions, 20 random restarts, stress value 0.063. Gene expression (arbitrary fluorescence units) was $\log_2$ transformed, normalized to reference gene expression, and multiplied by −1. Stations are organized from south (47, top) to north (102, bottom). Gene expression was not measured at Stn 113

species composition and physiological responses of each species to environmental gradients would aid in predicting future *Calanus* population responses. Overall, we found the population to be surprisingly homogeneous throughout the study range. The *Calanus* population was almost entirely composed of *Calanus glacialis*, i.e. our hypothesis that the population would exhibit a gradient from *C. marshallae* in the south to *C. glacialis* in the north was not supported. Similarly, we did not see latitudinal differences in prosome size, oil sac fullness, or lipid-related gene expression. Instead, we identified 1 southern station (Stn 66, near the Pribilof Islands) where the *C. glacialis* were larger and exhibited lower oil sac fullness and higher expression of lipid synthesis genes. Based on the fact that *in situ* gene expression differences were small relative to large decreases in lipid storage genes during shipboard incubations, we concluded that the population was still actively feeding and storing lipid in preparation for diapause. The minimal variation in prosome size, oil sac content, and gene expression across the focal stations suggests that through vertical migration, most of the *C. glacialis* that survived to the C5 stage experienced overall favorable growth conditions, albeit with some patchiness across stations.

The morphologically similar *C. marshallae* and *C. glacialis* co-occur in the Bering Sea, but we found the specimens analyzed to be overwhelmingly composed of *C. glacialis*. The 2 *C. marshallae* identified both came from a northern focal station. This was somewhat surprising because *C. marshallae* is abundant within the Gulf of Alaska (Frost 1974) and might be expected to be more common in the southern part of the Bering Sea relative to the predominantly Arctic *C. glacialis*. Because our study was focused primarily on characterizing gene expression patterns, individual copepods in good condition were rapidly sorted and preserved, which may have resulted in some bias toward the larger *C. glacialis*. To our knowledge, hybridization between *C. marshallae* and *C. glacialis* has not been documented, but our study was not specifically designed to detect hybrids, and we cannot discount that they may occur within the region. In addition, 2 distinct *C. glacialis* lineages exist, one of which is primarily found in the Bering Sea and the other in the Arctic (Nelson et al. 2009), but these were not discriminated in our study. Because *C. marshallae* and *C. glacialis* are often combined into 1 taxonomic group in ecological studies within the Bering Sea, very little is known regarding how distributions of species and populations have changed over time, and their ecophysiological differences are unknown. It seems likely that these lineages will exhibit distinct responses to changes in environmental conditions, so understanding this variability would improve efforts to model and predict future *Calanus* abundance.

Overall, the observed morphometric patterns were surprisingly similar, with no evidence for a hypothesized trend toward increasing size at northern stations. In field-based studies of *Calanus* spp., larger body size is typically correlated with colder temperatures (e.g. Wilson et al. 2015), though food availability during development can also affect body size (Campbell et al. 2001, Horne et al. 2016). We did find marked temperature differences between the north and south, particularly at depth; thus, we expected to see differences in prosome size. Instead, we found no clear patterns in prosome size or oil sac fullness along the 70 m isobath. Interestingly, *Calanus* from Stn 66 had large prosomes but low oil sac fullness. High total and large-fraction chl *a* and relatively high surface nutrients have been observed in late summer in this area due to the influx of nutrients along the middle front (~100 m isobath) and intrusions from the Pribilof Canyon, which incises the shelf in this region

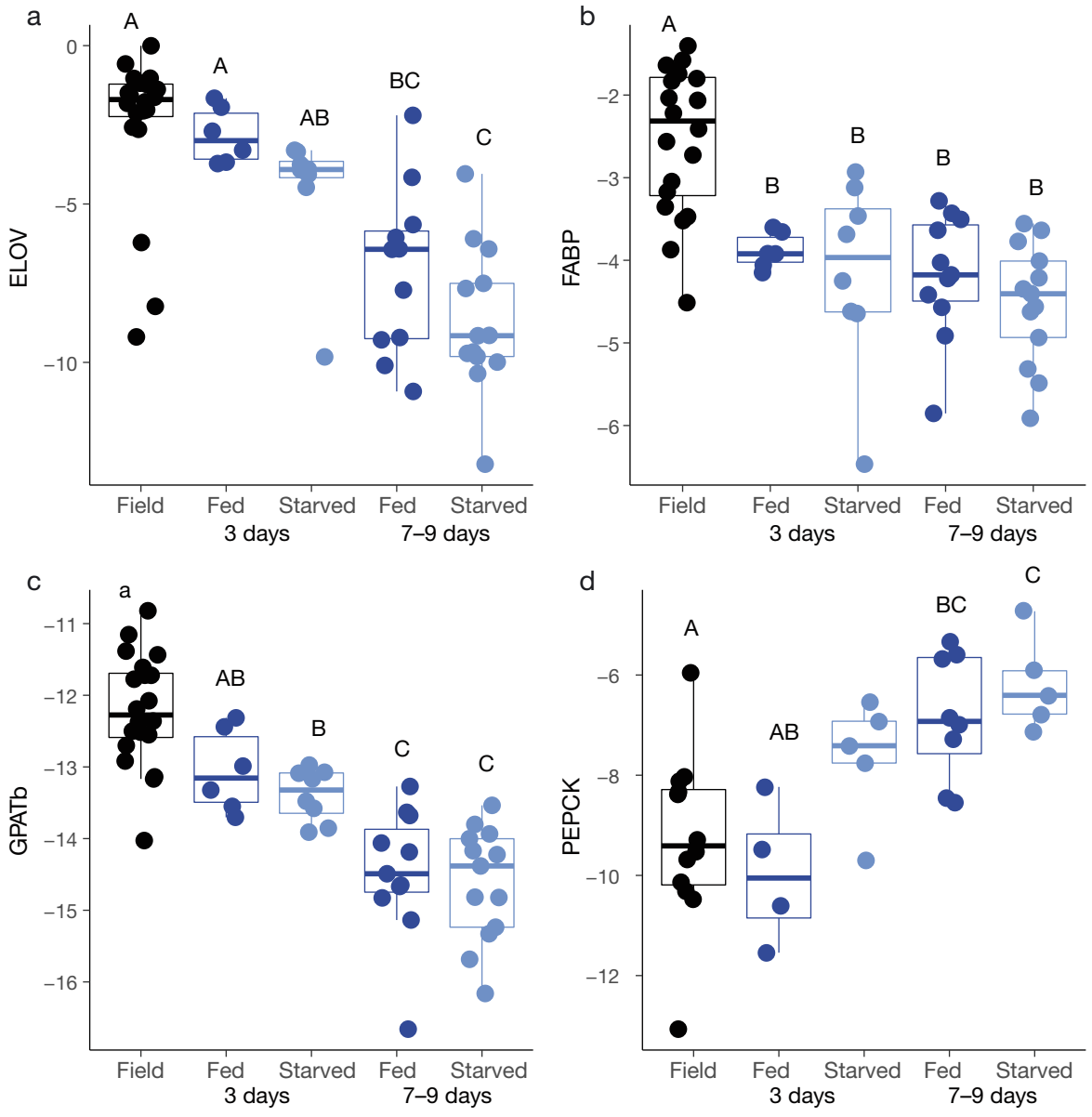

Fig. 10. Expression of metabolic genes from *Calanus glacialis* C5 copepodites collected from the field or incubated for varying periods (3 d, 7–9 d) with natural microplankton (Fed) or in filtered seawater (Starved). Genes shown are (a) ELOV, (b) FABP, (c) GPATb, and (d) PEPCK.Gene expression was $\log_2$ transformed and normalized prior to plotting and analysis (see Section 2.6). Boxplots show the first and third quartiles, with a line showing the median; individual measurements are displayed as horizontally jittered points. Uppercase letters indicate statistically distinct groups ($p < 0.05$; Games-Howell test). Treatments not sharing a common letter are significantly different, and treatments with no letters are not different from any others

(Eisner et al. 2016). High primary production and high abundances of seabirds and fur seals have also been observed in the tidally mixed waters adjacent to the Pribilof Islands (Byrd et al. 2008, Call et al. 2008, Hunt et al. 2008, Jahncke et al. 2008, Sambrotto et al. 2008). Therefore, the lack of a north–south gradient in morphometric patterns was perhaps not surprising, as the system is complicated by a variety of factors, including advection (generally northwestward) and cross-shelf exchange, that may result in more patchiness than may be predicted in a less advective system (Stabeno et al. 2010, Stabeno & Bell 2019). These indications of patchiness argue for examining copepods from a larger number of stations in future studies to resolve any spatial patterns.

Expression of a suite of lipid-related genes was measured in copepods collected from 4 focal stations, 2 of which were located in the northern cold pool and 2 in the warmer water to the south. As with morphometric data, we did not find evidence of north–south

gradients in expression of particular genes. Instead, we found elevated expression of lipid storage genes at Stn 66, which is consistent with the lower oil sac fullness at that station. When pooling the data from all focal stations, expression patterns of ELOV, FABP, and GPATb were positively correlated with one another, which presumably represents the related roles of these genes in lipid synthesis and storage. This interpretation is supported by studies of *C. finmarchicus*, in which FAPB and ELOV homologs show correlated expression that is upregulated early in the C5 stage of cultured animals and in field-collected C5 copepodites preparing for diapause (Tarrant et al. 2008, 2014, Häfker et al. 2018b). In addition, ELOV expression is negatively correlated with fractional fullness in both species (i.e. ELOV expression is high when the oil sac is small relative to body size). Also supporting a role in lipid storage, the GPATb homolog in *C. finmarchicus* is predominantly expressed during the lipid-storing C4 and C5 stages (Lenz et al. 2014). In contrast to the lipid storage genes, PEPCK was positively correlated with Lipase and negatively correlated with ELOV, FABP, and GPATb. This is consistent with roles of PEPCK and intracellular lipases in catabolizing energy stores. Based on recently published observations in *C. finmarchicus* (Häfker et al. 2018a,b), we predict that PEPCK expression would increase later in the fall after the copepods have entered into diapause.

Overall, the morphological and molecular measurements together suggest that despite the north–south temperature gradient, the *C. glacialis* population along the 70 m isobath had experienced similar ambient conditions and was preparing to enter diapause. Both advection and copepod behavior may have contributed to this relative homogeneity. For example, a large proportion of the *C. glacialis* C5 copepodites may have completed early development in regions of springtime productivity (e.g. associated with ice retreat in the northern Bering Sea) and seeded other areas through advection. Later copepodite stages undergo diel vertical migration (Schabetsberger et al. 2000), and this may have allowed *C. glacialis* in areas with different vertical oceanographic profiles to select similarly favorable growth conditions (Coyle & Gibson 2017). An alternative explanation is that through physiological plasticity, *C. glacialis* may have been able to achieve similar morphology and lipid storage under a variety of environmental conditions. In future studies, this possibility could be explored by comprehensive transcriptomic profiling or direct assessment of other physiological parameters.

The observed gene expression and morphology patterns were not related to differences in chl *a* or *Calanus* abundance. Total chl *a* is not necessarily a good proxy for prey availability for *C. glacialis* and *C. marshallae*, which selectively feed on larger phytoplankton and microzooplankton (Campbell et al. 2016). Neither microzooplankton abundance nor large phytoplankton were quantified at the focal stations; however, size-fractionated chl *a* measurements at a subset of stations along the 70 m isobath revealed that higher total chl *a* in the south was associated with a higher proportion of the large (>10 µm) size fraction (Duffy-Anderson et al. 2017). In general, there has been a positive association between total and large size fraction chl *a* during late summer on the middle shelf in the eastern Bering Sea (Eisner et al. 2016). Quantification of size-fractionated chl *a* and microzooplankton abundance throughout the growing season would be necessary to identify the relationships between prey availability and physiological status of *Calanus*. As an example of the utility of this approach, Roncalli et al. (2019) found that springtime expression of metabolic genes in female *Neocalanus flemingeri* varied along a strong gradient in chl *a* contained in large (>20 µm) cells. While we observed more than 10-fold variation in *Calanus* abundance across focal stations, the differences in gene expression and lipid accumulation were modest. This suggests that at all focal stations, the copepods that survived the early developmental stages were likely experiencing ambient food conditions that were conducive to lipid accumulation. This interpretation is supported by the rapid decline in expression of lipid storage genes during shipboard experiments. The strong effects of captivity and modest effects of feeding treatment indicated that the experimental conditions were suboptimal, and areas for improvement include reducing the culture density and utilizing a plankton wheel. Still, the directions of gene expression changes were consistent with the inferred roles of ELOV, FABP, and GPATb as lipid storage markers and PEPCK as a catabolic marker and suggest that these markers can be sensitive to short-term changes in food availability. Contrasting gene expression between the field-collected and experimental samples further supports the interpretation that the field population in general was still actively feeding and storing lipid.

In this study, we found a population of *Calanus* C5 copepodites that consisted of *C. glacialis* individuals exhibiting similar morphological and physiological characteristics despite being collected over a varying environmental gradient. We measured expression of

a small number of genes selected *a priori*. In the future, more insight could be gained by full transcriptional profiling (as in, e.g., Roncalli et al. 2019), which is becoming increasingly affordable with decreasing sequencing costs and new methods (Lohman et al. 2016). The results provide a snapshot of a population preparing to enter diapause and suggest that copepods that survive to the C5 stage are able to accumulate lipids across a patchwork of local conditions. Therefore, population declines during warm years (Eisner et al. 2018, Kimmel et al. 2018) may not have been driven by conditions during the later growth stages when lipid accumulation occurs. This is consistent with the results of an individual-based model of *Calanus* development in the eastern Bering Sea, which found that *Calanus* can achieve maximum size during both warm and cold conditions (Coyle & Gibson 2017). However, the modelling study also suggested that higher temperatures accelerate *Calanus* metabolic rates, which may result in exhausting lipid reserves during diapause and subsequent population decline during prolonged warm conditions. More data are clearly needed to compare *Calanus* physiology between warm and cold years, including measurements during diapause and immediately after exit, and gene expression profiling may prove a powerful tool for this evaluation.

Acknowledgements. We thank the captain and crew of the NOAA ship 'Oscar Dyson'. Robert Campbell and Celia Gelfman generously shared 16S genotyping protocols. We thank Sam Laney for logistical advice and the loan of sampling equipment and Mark Baumgartner for advice on image analysis and the loan of camera equipment. We thank George Hunt for insightful discussion and encouragement. We appreciate reviews by Cody Pinger, Adam Spear, Rob Suryan, Wes Larson, and 2 anonymous reviewers. We are grateful for the assistance from NOAA's Ecosystems and Fisheries Oceanography Coordinated Investigations (EcoFOCI) scientists in field sampling and analysis of CTD, chl *a*, and zooplankton abundance measurements. The scientific results and conclusions, as well as any views or opinions expressed herein, are those of the authors and do not necessarily reflect those of NOAA or the Department of Commerce. This is contribution EcoFOCI-1000.

LITERATURE CITED

Andrews AG, Cook MA, Siddon E, Dimond A (2019) Prey quality provides a leading indicator of energetic content for age-0 walleye pollock. In: Siddon E, Zador S (eds) Ecosystem status report 2019: eastern Bering Sea. North Pacific Fishery Management Council, Anchorage, AK, p 87–89

Baier CT, Napp JM (2003) Climate-induced variability in *Calanus marshallae* populations. J Plankton Res 25:771–782

Bailey A, De Wit P, Thor P, Browman HI and others (2017) Regulation of gene expression is associated with tolerance of the Arctic copepod *Calanus glacialis* to CO_2-acidified sea water. Ecol Evol 7:7145–7160

Banas NS, Møller EF, Nielsen TG, Eisner LB (2016) Copepod life strategy and population viability in response to prey timing and temperature: testing a new model across latitude, time, and the size spectrum. Front Mar Sci 3:225

Bucklin A, Frost B, Kocher T (1995) Molecular systematics of six *Calanus* and three *Metridia* species (Calanoida: Copepoda). Mar Biol 121:655–664

Byrd GV, Schmutz JA, Renner HM (2008) Contrasting population trends of piscivorous seabirds in the Pribilof Islands: a 30-year perspective. Deep Sea Res II 55: 1846–1855

Call KA, Ream RR, Johnson D, Sterling JT, Towell RG (2008) Foraging route tactics and site fidelity of adult female northern fur seal (*Callorhinus ursinus*) around the Pribilof Islands. Deep Sea Res II 55:1883–1896

Campbell RG, Wagner MM, Teegarden GJ, Boudreau CA, Durbin EG (2001) Growth and development rates of the copepod *Calanus finmarchicus* reared in the laboratory. Mar Ecol Prog Ser 221:161–183

Campbell RG, Ashjian CJ, Sherr EB, Sherr BF and others (2016) Mesozooplankton grazing during spring sea-ice conditions in the eastern Bering Sea. Deep Sea Res II 134:157–172

Cleary AC, Søreide JE, Freese D, Niehoff B, Gabrielsen TM (2017) Feeding by *Calanus glacialis* in a high arctic fjord: potential seasonal importance of alternative prey. ICES J Mar Sci 74:1937–1946

Coyle K, Gibson G (2017) *Calanus* on the Bering Sea shelf: probable cause for population declines during warm years. J Plankton Res 39:257–270

Coyle KO, Eisner LB, Mueter FJ, Pinchuk AI and others (2011) Climate change in the southeastern Bering Sea: impacts on pollock stocks and implications for the oscillating control hypothesis. Fish Oceanogr 20:139–156

Daase M, Falk-Petersen S, Varpe O, Darnis G and others (2013) Timing of reproductive events in the marine copepod *Calanus glacialis:* a pan-Arctic perspective. Can J Fish Aquat Sci 70:871–884

Duffy-Anderson JT, Stabeno PJ, Siddon EC, Andrews AG and others (2017) Return of warm conditions in the southeastern Bering Sea: phytoplankton — fish. PLOS ONE 12:e0178955

Eisner LB, Napp JM, Mier KL, Pinchuk AI, Andrews AG (2014) Climate-mediated changes in zooplankton community structure for the eastern Bering Sea. Deep Sea Res II 109:157–171

Eisner LB, Gann JC, Ladd C, Cieciel KD, Mordy CW (2016) Late summer/early fall phytoplankton biomass (chlorophyll *a*) in the eastern Bering Sea: spatial and temporal variations and factors affecting chlorophyll *a* concentrations. Deep Sea Res II 134:100–114

Eisner LB, Pinchuk AI, Kimmel DG, Mier KL, Harpold CE, Siddon EC (2018) Seasonal, interannual, and spatial patterns of community composition over the eastern Bering Sea shelf in cold years. Part I: zooplankton. ICES J Mar Sci 75:72–86

Evans LE, Hirst AG, Kratina P, Beaugrand G (2020) Temperature-mediated changes in zooplankton body size: large scale temporal and spatial analysis. Ecography 43: 581–590

Falk-Petersen S, Mayzaud P, Kattner G, Sargent JR (2009) Lipids and life strategy of Arctic *Calanus.* Mar Biol Res 5: 18–39

Fissel B, Dalton M, Garber-Yonts B, Haynie A and others (2017) Stock assessment and fishery evaluation report for the groundfish fisheries of the Gulf of Alaska and Bering Sea/Aleutian Island area: economic status of the groundfish fisheries off Alaska, 2016. Alaska Fisheries Science Center, National Marine Fisheries Service, National Oceanic and Atmospheric Administration, Seattle, WA

Frost BW (1974) *Calanus marshallae,* a new species of calanoid copepod closely allied to the sibling species *C. finmarchicus* and *C. glacialis.* Mar Biol 26:77–99

Grebmeier JM, Overland JE, Moore SE, Farley EV and others (2006) A major ecosystem shift in the northern Bering Sea. Science 311:1461–1464

Häfker NS, Teschke M, Hüppe L, Meyer B (2018a) *Calanus finmarchicus* diel and seasonal rhythmicity in relation to endogenous timing under extreme polar photoperiods. Mar Ecol Prog Ser 603:79–92

Häfker NS, Teschke M, Last KS, Pond DW, Hüppe L, Meyer B (2018b) *Calanus finmarchicus* seasonal cycle and diapause in relation to gene expression, physiology, and endogenous clocks. Limnol Oceanogr 63:2815–2838

Hakanson JL (1984) The long and short term feeding condition in field-caught *Calanus pacificus*, as determined from the lipid content. Limnol Oceanogr 29:794–804

Halvorsen E (2015) Significance of lipid storage levels for reproductive output in the Arctic copepod *Calanus hyperboreus.* Mar Ecol Prog Ser 540:259–265

Hansen BH, Altin D, Øverjordet IB, Jager T, Nordtug T (2013) Acute exposure of water soluble fractions of marine diesel on Arctic *Calanus glacialis* and boreal *Calanus finmarchicus*: effects on survival and biomarker response. Sci Total Environ 449:276–284

Harrell FE Jr, Dupont MC (2006) The Hmisc package. R package version 3:3. https://hbiostat.org/R/Hmisc/

Hermann AJ, Gibson GA, Cheng W, Ortiz I and others (2019) Projected biophysical conditions of the Bering Sea to 2100 under multiple emission scenarios. ICES J Mar Sci 76:1280–1304

Hobbs L, Banas NS, Cottier FR, Berge J, Daase M (2020) Eat or sleep: availability of winter prey explains mid-winter and spring activity in an arctic *Calanus* population. Front Mar Sci 7:541564

Horne CR, Hirst AG, Atkinson D, Neves A, Kiørboe T (2016) A global synthesis of seasonal temperature–size responses in copepods. Glob Ecol Biogeogr 25:988–999

Hunt GL Jr, Stabeno PJ, Strom S, Napp JM (2008) Patterns of spatial and temporal variation in the marine ecosystem of the southeastern Bering Sea, with special reference to the Pribilof Domain. Deep Sea Res II 55:1919–1944

Hunt GL Jr, Yasumiishi EM, Eisner LB, Stabeno PJ, Decker MB (2020) Climate warming and the loss of sea ice: the impact of sea-ice variability on the southeastern Bering Sea pelagic ecosystem. ICES J Mar Sci 2020:fsaa206

Ikeda T, Kanno Y, Ozaki K, Shinada A (2001) Metabolic rates of epipelagic marine copepods as a function of body mass and temperature. Mar Biol 139:587–596

Jahncke J, Vlietstra LS, Decker MB, Hunt GL Jr (2008) Marine bird abundance around the Pribilof Islands: a multiyear comparison. Deep Sea Res II 55:1809–1826

Kimmel DG, Eisner LB, Wilson MT, Duffy-Anderson JT (2018) Copepod dynamics across warm and cold periods in the eastern Bering Sea: implications for walleye pollock (*Gadus chalcogrammus*) and the oscillating control hypothesis. Fish Oceanogr 27:143–158

Kiørboe T, Hirst AG (2008) Optimal development time in pelagic copepods. Mar Ecol Prog Ser 367:15–22

Lee RF, Hagen W, Kattner G (2006) Lipid storage in marine zooplankton. Mar Ecol Prog Ser 307:273–306

Lenz PH, Roncalli V, Hassert RP, Wu LS, Cieslak MC, Hartline DK, Christie AE (2014) *De novo* assembly of a transcriptome for *Calanus finmarchicus* (Crustacea, Copepoda) — the dominant zooplankter of the North Atlantic Ocean. PLOS ONE 9:e88589

Lindeque P, Hay S, Heath M, Ingvarsdottir A, Rasmussen J, Smerdon G, Waniek JJ (2006) Integrating conventional microscopy and molecular analysis to analyse the abundance and distribution of four *Calanus* congeners in the North Atlantic. J Plankton Res 28:221–238

Lohman BK, Weber JN, Bolnick DI (2016) Evaluation of TagSeq, a reliable low-cost alternative for RNAseq. Mol Ecol Resour 16:1315–1321

Lomas MW, Eisner LB, Gann J, Baer SE, Mordy CW, Stabeno PJ (2020) Time-series of direct primary production and phytoplankton biomass in the southeastern Bering Sea: responses to cold and warm stanzas. Mar Ecol Prog Ser 642:39–54

Mayzaud P, Falk-Petersen S, Noyon M, Wold A, Boutoute M (2016) Lipid composition of the three co-existing *Calanus* species in the Arctic: impact of season, location and environment. Polar Biol 39:1819–1839

Miksis-Olds JL, Stabeno PJ, Napp JM, Pinchuk AI, Nystuen JA, Warren JD, Denes SL (2013) Ecosystem response to a temporary sea ice retreat in the Bering Sea: winter 2009. Prog Oceanogr 111:38–51

Miller C, Crain J, Morgan C (2000) Oil storage variability in *Calanus finmarchicus.* ICES J Mar Sci 57:1786–1799

National Marine Fisheries Service (2020) Fisheries of the United States 2018. US Department of Commerce, NOAA Current Fishery Statistics No. 2018. https://www.fisheries.noaa.gov/national/commercial-fishing/fisheries-united-states-2018

Nelson RJ, Carmack EC, McLaughlin FA, Cooper GA (2009) Penetration of Pacific zooplankton into the western Arctic Ocean tracked with molecular population genetics. Mar Ecol Prog Ser 381:129–138

Oksanen JF, Blanchet G, Friendly M, Kindt R and others (2019) vegan: community ecology package. R package version 2.5-6. https://CRAN.R-project.org/package=vegan

Palanker L, Tennessen JM, Lam G, Thummel CS (2009) *Drosophila* HNF4 regulates lipid mobilization and β-oxidation. Cell Metab 9:228–239

Palumbi SR, Benzie J (1991) Large mitochondrial DNA differences between morphologically similar penaeid shrimp. Mol Mar Biol Biotechnol 1:27–34

Peters G (2018) userfriendlyscience: quantitative analysis made accessible. R package version 0.7.2. , https://userfriendlyscience.com

Plourde S, Campbell RG, Ashjian CJ, Stockwell DA (2005) Seasonal and regional patterns in egg production of *Calanus glacialis/marshallae* in the Chukchi and Beaufort seas during spring and summer, 2002. Deep Sea Res II 52:3411–3426

Poelchau MF, Reynolds JA, Elsik CG, Denlinger DL, Armbruster PA (2013) Deep sequencing reveals complex mechanisms of diapause preparation in the invasive mosquito, *Aedes albopictus.* Proc Biol Sci 280:20130143

Core Team (2020) R: a language and environment for statistical computing. R Foundation for Statistical Computing, Vienna. www.R-project.org

Ramakers C, Ruijter JM, Deprez RHL, Moorman AF (2003)

Assumption-free analysis of quantitative real-time polymerase chain reaction (PCR) data. Neurosci Lett 339:62–66

Ramos AA, Weydmann A, Cox CJ, Canario AVM, Serrao EA, Pearson GA (2015) A transcriptome resource for the copepod *Calanus glacialis* across a range of culture temperatures. Mar Genomics 23:27–29

Rey-Rassat C, Irigoien X, Harris R, Carlotti F (2002) Energetic cost of gonad development in *Calanus finmarchicus* and *C. helgolandicus*. Mar Ecol Prog Ser 238:301–306

Rivera-Pérez C (2015) Marine invertebrate lipases: comparative and functional genomic analysis. Comp Biochem Physiol Part D Genomics Proteomics 15:39–48

Rivera-Pérez C, García-Carreno FL, Saborowski R (2011) Purification and biochemical characterization of digestive lipase in whiteleg shrimp. Mar Biotechnol (NY) 13: 284–295

Roncalli V, Cieslak MC, Germano M, Hopcroft RR, Lenz PH (2019) Regional heterogeneity impacts gene expression in the subarctic zooplankter *Neocalanus flemingeri* in the northern Gulf of Alaska. Commun Biol 2:324

Sambrotto RN, Mordy C, Zeeman SI, Stabeno PJ, Macklin SA (2008) Physical forcing and nutrient conditions associated with patterns of chl *a* and phytoplankton productivity in the southeastern Bering Sea during summer. Deep Sea Res II 55:1745–1760

Saumweber WJ, Durbin EG (2006) Estimating potential diapause duration in *Calanus finmarchicus*. Deep Sea Res II 53:2597–2617

Schabetsberger R, Brodeur R, Ciannelli L, Napp J, Swartzman G (2000) Diel vertical migration and interaction of zooplankton and juvenile walleye pollock (*Theragra chalcogramma*) at a frontal region near the Pribilof Islands, Bering Sea. ICES J Mar Sci 57:1283–1295

Sigler MF, Stabeno PJ, Eisner LB, Napp JM, Mueter FJ (2014) Spring and fall phytoplankton blooms in a productive subarctic ecosystem, the eastern Bering Sea, during 1995–2011. Deep Sea Res II 109:71–83

Smolina I, Kollias S, Poortvliet M, Nielsen TG and others (2014) Genome- and transcriptome-assisted development of nuclear insertion/deletion markers for *Calanus* species (Copepoda: Calanoida) identification. Mol Ecol Resour 14:1072–1079

Smolina I, Kollias S, Møller EF, Lindeque P, Sundaram AYM, Fernandes JMO, Hoarau G (2015) Contrasting transcriptome response to thermal stress in two key zooplankton species, *Calanus finmarchicus* and *C. glacialis*. Mar Ecol Prog Ser 534:79–93

Søreide JE, Leu E, Berge J, Graeve M, Falk-Petersen S (2010) Timing of blooms, algal food quality and *Calanus glacialis* reproduction and growth in a changing Arctic. Glob Change Biol 16:3154–3163

Spacht DE, Teets NM, Denlinger DL (2018) Two isoforms of *Pepck* in *Sarcophaga bullata* and their distinct expression profiles through development, diapause, and in response to stresses of cold and starvation. J Insect Physiol 111:41–46

Stabeno PJ, Bell SW (2019) Extreme conditions in the Bering Sea (2017–2018): record-breaking low sea-ice extent. Geophys Res Lett 46:8952–8959

Stabeno P, Napp J, Mordy C, Whitledge T (2010) Factors influencing physical structure and lower trophic levels of the eastern Bering Sea shelf in 2005: sea ice, tides and winds. Prog Oceanogr 85:180–196

Stabeno PJ, Farley EV Jr, Kachel NB, Moore S and others (2012) A comparison of the physics of the northern and southern shelves of the eastern Bering Sea and some implications for the ecosystem. Deep Sea Res II 65–70: 14–30

Stevens CJ, Deibel D, Parrish CC (2004) Incorporation of bacterial fatty acids and changes in a wax ester-based omnivory index during a long-term incubation experiment with *Calanus glacialis* Jaschnov. J Exp Mar Biol Ecol 303:135–156

Strasburger WW, Hillgruber N, Pinchuk AI, Mueter FJ (2014) Feeding ecology of age-0 walleye pollock (*Gadus chalcogrammus*) and Pacific cod (*Gadus macrocephalus*) in the southeastern Bering Sea. Deep Sea Res II 109: 172–180

Tarrant AM, Baumgartner MF, Verslycke T, Johnson CL (2008) Differential gene expression in diapausing and active *Calanus finmarchicus* (Copepoda). Mar Ecol Prog Ser 355:193–207

Tarrant AM, Baumgartner MF, Hansen BH, Altin D, Nordtug T, Olsen AJ (2014) Transcriptional profiling of reproductive development, lipid storage and molting throughout the last juvenile stage of the marine copepod *Calanus finmarchicus*. Front Zool 11:91

Thor P, Bailey A, Halsband C, Guscelli E, Gorokhova E, Fransson A (2016) Seawater pH predicted for the year 2100 affects the metabolic response to feeding in copepodites of the Arctic copepod *Calanus glacialis*. PLOS ONE 11:e0168735

Vogedes D, Varpe Ø, Søreide JE, Graeve M, Berge J, Falk-Petersen S (2010) Lipid sac area as a proxy for individual lipid content of arctic calanoid copepods. J Plankton Res 32:1471–1477

Wendel AA, Lewin TM, Coleman RA (2009) Glycerol-3-phosphate acyltransferases: rate limiting enzymes of triacylglycerol biosynthesis. Biochim Biophys Acta Lipid Lipid Met 1791:501–506

Wilson RJ, Speirs DC, Heath MR (2015) On the surprising lack of differences between two congeneric calanoid copepod species, *Calanus finmarchicus* and *C. helgolandicus*. Prog Oceanogr 134:413–431

Editorial responsibility: Sigrun Jónasdóttir, Charlottenlund, Denmark
Reviewed by: 2 anonymous referees

Submitted: March 2, 2021
Accepted: July 5, 2021
Proofs received from author(s): September 10, 2021